

# Effect of Process-Product Parameters on Strength of 3D Printed Primitive Scaffold Structures



Author

**Abdul Moiz Siddiqui**

Regn Number: 318685

Supervisor

**DR. Sajid Ullah Butt**

DEPARTMENT OF MECHANICAL ENGINEERING  
COLLEGE OF ELECTRICAL & MECHANICAL ENGINEERING  
NATIONAL UNIVERSITY OF SCIENCES AND TECHNOLOGY  
ISLAMABAD  
NOVEMBER, 2022

# **Effect of Process-Product Parameters on Strength of 3D Printed Primitive Scaffold Structures**

Author

**Abdul Moiz Siddiqui**

Regn Number: 318685

A thesis submitted in partial fulfillment of the requirements for the degree of  
MS Mechanical Engineering

Thesis Supervisor:

**DR. Sajid Ullah Butt**

Thesis Supervisor's Signature: \_\_\_\_\_

DEPARTMENT OF MECHANICAL ENGINEERING  
COLLEGE OF ELECTRICAL & MECHANICAL ENGINEERING  
NATIONAL UNIVERSITY OF SCIENCES AND TECHNOLOGY,  
ISLAMABAD  
NOVEMBER, 2022

## Declaration

I certify that this research work titled "*Effect of process-product parameters on strength of 3D printed primitive scaffold structures*" is my own work. The work has not been presented elsewhere for assessment. The material that has been used from other sources has been properly acknowledged/referred.

Signature of Student

Abdul Moiz Siddiqui

318685

## Language Correctness Certificate

This thesis has been read by an English expert and is free of typing, syntax, semantic, grammatical and spelling mistakes. The thesis is also according to the format given by the university.

---

Signature of Student

Abdul Moiz Siddiqui

318685

MS-ME-19

---

Signature of Supervisor

DR. Sajid Ullah Butt

## Copyright Statment

- Copyright in the text of this thesis rests with the student author. Copies (by any process) either in full, or of extracts, may be made only in accordance with instructions given by the author and lodged in the Library of College of E&ME, NUST. Details may be obtained by the Librarian. This page must form part of any such copies made. Further copies (by any process) may not be made without the permission (in writing) of the author.
- The ownership of any intellectual property rights which may be described in this thesis is vested in NUST College of E&ME, subject to any prior agreement to the contrary, and may not be made available for use by third parties without the written permission of the College of E&ME, which will prescribe the terms and conditions of any such agreement.
- Further information on the conditions under which disclosures and exploitation may take place is available from the Library of College of E&ME, NUST, Rawalpindi.

## **Acknowledgments**

I am thankful to my Creator Allah Subhana-Watala to have guided me throughout this work at every step and for every new thought which You set up in my mind to improve it. Indeed I could have done nothing without Your priceless help and guidance. Whosoever helped me throughout the course of my thesis, whether my parents or any other individual was Your will, so indeed none be worthy of praise but You.

I am profusely thankful to my beloved parents who raised me when I was not capable of walking and continued to support me throughout in every department of my life.

I would also like to express special thanks to my supervisor Dr. Sajid Ullah Butt for his help throughout my thesis.

I would also like to thank Dr. Aamer Ahmed Baqai and Dr. Uzair Khaliq uz Zaman for being on my thesis guidance and evaluation committee.

Finally, I would like to express my gratitude to all the individuals who have rendered valuable assistance to my study.

*Dedicated to my exceptional parents and adored siblings whose  
tremendous support and cooperation led me to this wonderful  
accomplishment*

## Abstract

3D printing by FDM is latest technique, the world using for manufacturing complex geometric parts. Materials like Acrylonitrile Butadiene Styrene (ABS), Polylactic Acid (PLA) are commonly used to carry out this method. This study is based on the effect of process-product parameters on strength of 3D printed scaffold structures. 3D printed scaffold structures have a lot of applications in biomedical engineering. As there are a lot of supporting structures of cellular interactions that assists in growth & development of new tissues that replace the damaged tissues present in the body.

Primitive scaffold structure is one of the Triply Periodic Minimal Surfaces (TPMS) structures. In this work, Taguchi Design of Experiment (DOE)  $L_{27}$  array is used, for performing number of experiments with four different process-product parameters such as raster angle, unit cell size, layer thickness & extrusion temperature having three level of input values. Optimized process parameters are calculated on the basis of these optimized parameters and a new part is fabricated which have much better compressive strength properties.

**Keywords:** 3D printing, Gyroid Structures, PLA Scaffold, DOE, Tissue Engineering, Compressive Strength.



# Table of Contents

<b>Declaration</b> .....	<b>i</b>
<b>Language Correctness Certificate</b> .....	<b>ii</b>
<b>Copyright Statment</b> .....	<b>iii</b>
<b>Acknowledgments</b> .....	<b>iv</b>
<b>Abstract</b> .....	<b>vi</b>
<b>List of Abbreviations</b> .....	<b>xi</b>
<b>CHAPTER 1: INTRODUCTION</b> .....	<b>12</b>
1.1. Background .....	12
1.2. Motivation.....	12
1.3. Research Objectives .....	13
1.4. Thesis Outline.....	13
<b>CHAPTER 2: LITERATURE REVIEW</b> .....	<b>15</b>
2.1. 3D Printing Technology Overview .....	15
2.2. Types of Scaffold Structures .....	15
2.2.1. Primitive structure .....	15
2.2.2. Gyroid-structures .....	15
2.2.3. TPMS-structures.....	15
2.2.4. The diamond cubic.....	15
2.3. Primitive Structures .....	16
2.4. 3D Printing CAD Interface .....	19
2.5. Fused Deposition Modeling (FDM) .....	20
2.6. FDM Process Parameters .....	21
2.6.1. Orientation:.....	21
2.6.2. Layer thickness:.....	21
It is a thickness of layer deposited by nozzle and depends upon the type of nozzle used. ....	21
2.6.3. Raster angle: .....	21
2.6.4. Part raster width: .....	21
2.6.5. Raster to raster gap:.....	21
2.6.6. Extrusion Temperature: .....	21
2.6.7. Unit cell size: .....	21
2.7. 3D Printed Cellular Structures for Tissue Engineering .....	22
2.8. Research Gap and Challenges .....	23
<b>CHAPTER 3: MATERIALS AND METHODS</b> .....	<b>25</b>

3.1. Methodology.....	25
3.2. Selection of Input Parameters .....	26
3.2.1. Raster Angle .....	26
3.2.2. Unit Cell Size.....	26
3.2.3. Layer thickness.....	26
3.2.4. Extrusion Temperature .....	27
3.3. Fabrication of Samples.....	28
3.4. Compression Testing Requirements and Specifications .....	31
<b>CHAPTER 4: RESULTS AND DISCUSSION.....</b>	<b>33</b>
4.1. Compression Tests Specimens.....	33
4.2. Statistical Analysis.....	35
4.2.1. Regression Analysis.....	35
4.3. Results and discussion .....	40
<b>CHAPTER 5: CONCLUSION .....</b>	<b>42</b>
5.1. Conclusion.....	42
5.2. Findings of This Study .....	42
5.3. Limitations of 3D Printing Machine Available for this Study .....	43
5.4. Scope of Future Studies .....	43
<b>REFERENCES .....</b>	<b>44</b>
<b>CERTIFICATE OF COMPLETENESS.....</b>	<b>46</b>

## List of Figures

<b>Figure 1-1:</b> Diagram of 3D printing process [21] .....	13
<b>Figure 2-1:</b> Primitive TPMS scaffold structure and unit cell [27] .....	16
<b>Figure 2-2:</b> Distribution of Additive Manufacturing (AM) from 2015 to 2019 in prototype manufacturing, production and research & educational industry [21] .....	18
<b>Figure 2-3:</b> Main uses of additive manufacturing (AM) technologies in different industries [21] .....	18
<b>Figure 2-4:</b> FDM process schematic diagram [25] .....	20
<b>Figure 2-5:</b> Input parameters that are influencing strength of structure.....	22
<b>Figure 2-6:</b> Repair of bone defects using bone tissue engineering scaffolds [26] .....	23
<b>Figure 3-1:</b> Different raster angles.....	26
<b>Figure 3-2:</b> Representation of extrusion width or layer thickness [28] .....	27
<b>Figure 3-3:</b> 3D printing "Crealty CR-10 Pro" machine setup.....	29
<b>Figure 3-4:</b> CAD models of primitive scaffold structures.....	29
<b>Figure 3-5:</b> 3D printed primitive scaffold 9 samples.....	31
<b>Figure 3-6:</b> Sample subjected to compression test .....	32
<b>Figure 4-1:</b> Strength graph of 27 samples.....	35
<b>Figure 4-2:</b> Main impact plots for compressive strength .....	36
<b>Figure 4-3:</b> Main effect plot for means and S/N ratio .....	37
<b>Figure 4-4:</b> Contour plot for max stress VS unit cell size, raster angle .....	38
<b>Figure 4-5:</b> Contour plot for max stress VS unit cell size, layer thickness .....	38
<b>Figure 4-6:</b> Contour plot for max stress vs unit cell size, extrusion temperature .....	38
<b>Figure 4-7:</b> Contour plot for max stress vs raster angle, extrusion temperature.....	39
<b>Figure 4-8:</b> Contour plot for max stress VS raster angle, layer thickness.....	39
<b>Figure 4-9:</b> Contour plot for max stress VS raster angle, unit cell size .....	39
<b>Figure 4-10:</b> Optimal factors values for maximum compressive strength .....	40
<b>Figure 4-11:</b> 28th sample having fabricated on base of optimized parameter using ANOVA.....	41
<b>Figure 4-12:</b> Strength comparison of 28th part and remaining 27 parts.....	41

## List of Table

<b>Table 2-1:</b> Available standard formats for rapid prototyping [21] .....	20
<b>Table 3-1:</b> Flow chart of methodology .....	25
<b>Table 3-2:</b> Varying values of FDM input process parameters.....	27
<b>Table 3-3:</b> Taguchi L <sub>27</sub> Orthogonal Array table.....	28
<b>Table 3-4:</b> Fixed FDM parameters of 3D printer.....	30
<b>Table 4-1:</b> Compression tests of all samples on UTM.....	33
<b>Table 4-2:</b> Stress test for all samples done on UTM.....	34
<b>Table 4-3:</b> P value.....	36

## List of Abbreviations

### Abbreviations

<b>FDM</b>	Fused Deposition Modeling
<b>3D</b>	Three Dimensional
<b>ABS</b>	Acrylonitrile Butadiene Styrene
<b>AM</b>	Additive Manufacturing
<b>CAD</b>	Computer Aided Design
<b>CAM</b>	Computer Aided Manufacturing
<b>DMLS</b>	Direct Metal Laser Sintering
<b>DOE</b>	Design of Experiment
<b>PLA</b>	Poly-lactic Acid
<b>RP</b>	Rapid Prototyping
<b>LOM</b>	Laminated Object Manufacturing
<b>SL</b>	Stereo Lithography
<b>SLS</b>	Selective Laser Sintering
<b>PEEK</b>	Polyether Ether Ketone
<b>PET</b>	Polyethylene Terephthalate

# CHAPTER 1: INTRODUCTION

## 1.1. Background

Rapid prototyping or AM is used for fabrication of 3D objects by using CAD models by a process which involves depositing one material layer onto the top of other layer [1]. Nowadays, additive manufacturing has been widely used because of its capability to fabricate complex parts [2]. Stereolithography (SLA) is an Additive Manufacturing technique which has been employed in polymer manufacturing [3], Fused Deposition Modeling (FDM) which uses polymer filaments. SLS includes the use of polymer powders. PLA is a thermoplastic material which is widely used as a filament in fused deposition process [4].

3D printed scaffolds are widely used to provide temporary support to the bone for growth of new tissues and for cell transmissions while replacing the damaged tissue cells which are present in the body [5]. The geometry of microcellular structures plays vital role in defining the characteristics of scaffold structures [6]. The primitive structure is one of the triply periodic minimal surfaces (TPMS) having good resemblance to the bone's structure & have been widely used in implantations of bones. TPMS are complicated in geometry & have no straight lines [7]. Designing the additive manufacturing's lattice structure has become very popular within few years mostly in biomedical engineering field [8].

Latest research likes in reducing the weight of the structure while increasing the strength [9]. Due to porosity involves in the design, mechanical properties has been changed. Although increasing mechanical properties while reducing weight of structure is a challenging task [10]. But Triply Periodic Minimal Surfaces (TPMS) have made that challenge possible to achieve best mechanical properties while dealing with light weight structure [11].

## 1.2. Motivation

3D printed polymer scaffolds have become one of the leading supporting structures for tissues engineering due to the large number of applications and their bio compliance. The use of polymers in compacted deposits has increased considerably. However the use of efficient polymers and compounds is now needed and growing rapidly.

FDM uses PLA, PEEK, PET, ABS, Nylon, etc. as raw material is heated and deposited layer by layer through nozzle to fabricate 3D structure. The diagram of FDM process is shown in Figure 1.1. 3D printer deposits the layer upon layer by extruding the heated or semi melted raw material according

to the CAD geometry, working from bottom up. Depending upon process product parameters, mechanical properties of structure may vary. Different parameters such as Raster angle, Raster width, unit cell size, printing temperature, printing pattern, layer thickness, nozzle temperature, nozzle diameter, printing speed, melting temperature, air gap & infill density can be varied to make 3D objects.

Primitive structure is fabricated using Taguchi Design of Experiment (DOE)  $L_{27}$  array method while considering process product parameters like extrusion temperature, raster angle, layer thickness, unit cell size. The aim of this research is to achieve maximum compressive strength of primitive scaffold structure while trying to make structure light weight and porous.

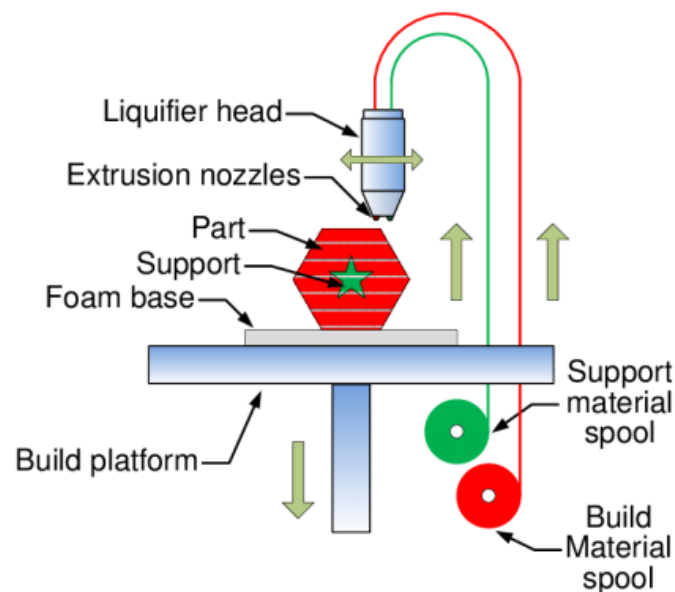


**Figure 1-1:** Diagram of 3D printing process [21]

### 1.3. Research Objectives

Main objectives of this study include:

- To study the effect of various input parameters on the strength of scaffold structure.
- For input parameters out of raster angle, layer width, unit cell size, contour, porosity, infill density, extrusion width, volume fraction I have chosen raster angle, unit cell size & layer width.
- To investigate effect of raster angle, unit cell size & layer width on compressive strength of PLA based primitive scaffold structure.

### 1.4. Thesis Outline

This report is categorized into five chapters. Chapter 1 includes the introduction of the additive manufacturing (AM) technology, its background and motivation to use FDM, additive manufacturing

process to fabricate scaffold structures for our study. Literature review of the 3D printing technology, CAD interface used in 3D printing process, FDM process, input and output process-product parameters are used in previous studies, 3D printing process are used in tissue engineering and literature gap regarding effect of FDM parameters on the compressive strength of 3D printed objects are discussed in Chapter 2. Materials and methods are presented in Chapter 3 and potential of TPMS, compression tests requirements and selection of process parameters depending upon their significance evident from literature were reported. Chapter 4 presents the results of compression tests & statistical analysis and discusses the significance of process parameters with the aid of P values and individual effect size for parameters. The thesis is concluded in Chapter 5 and future scope for parametric studies is presented to guide the researchers for further studies.



## CHAPTER 2: LITERATURE REVIEW

### 2.1. 3D Printing Technology Overview

3D printing is used for construction of a 3D object from a CAD model. It can be carried out in variety of processes in which material is coated layer-by-layer which solidified under computer control, with materials that are added together [1].

FDM is a excessively used technique for making 3D objects RP in a limited time. In this technique, the model is fabricated as a layer-by-layer deposition of melted material on a bed [1]. The effect of process-product parameters on strength of 3D printed primitive scaffold structures will be discussed in results section. FDM is cheap & easy-to-use additive manufacturing method by using which one can produce a structure of any shape [5].

Different parameters are associated with 3D printing which includes extrusion temperature, raster angle, layer thickness, infill pattern, infill deposition speed, porosity, unit cell size. Tissue engineering with respect to additive manufacturing has come up with an alternative technique to renew damaged organs & tissues by developing patient-specific substitutes that improve, restore or maintain tissue function. Scaffold structures are hollow and they can be fabricated by using 3D printing and used in tissue engineering.

### 2.2. Types of Scaffold Structures

There are different type of scaffold structures like primitive structure, diamond structure, TPMS structure & gyroid structure.

#### 2.2.1. Primitive-structure

Primitive structure consist of unit cell corresponding to single lattice point. Primitive structure has four holes per unit cell.

#### 2.2.2. Gyroid-structures

Gyroid structure has two layers per unit cell. It resembles with the microstructure of bone.

#### 2.2.3. TPMS-structures

Each unit cell is merged to make cubically symmetrical scaffold structure that contains periodic repetition of interconnected holes.

#### 2.2.4. The diamond cubic

Diamond cubic structure repeats the pattern of eight atoms that certain materials may acquire as they attached.

### 2.3. Primitive Structures

3D printed scaffold structures as shown in figure 2-1, mostly used for tissue repair and cell growth transmission in human body would allow for many cell types to grow. This technology can be used to boost up the repair of tissues that are complex like bone, which comprises of different unit cells.

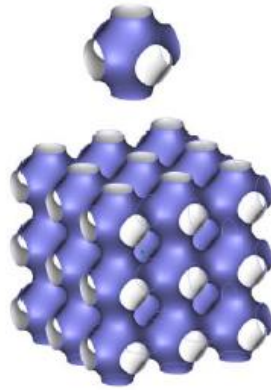


**Figure 2-1:** Primitive TPMS scaffold structure and unit cell [27]

The Primitive cell is a unit cell that be in tune with single lattice point. In most of the cases, full consistency of the crystal structure is not clear from schwarz cell; primitive surface is beneficial to soak up bone cell & nutrients.

The density of lattice cube can be expressed as the relative density as given in equation (1):

$$\rho = V_{\text{primitive}} / V_{\text{cube}} \quad (1)$$

where,  $V_{\text{primitive}}$  represents Volume of primitive lattice &  $V_{\text{cube}}$  represents Volume of solid cube. The relative density is controlled by unit cell size when the wall thickness is kept low. The porosity of primitive structures is given in equation (2):

$$\% \text{Porosity} = V_v / V_T \quad (2)$$

where,  $V_v$  indicates Volume of void in structure &  $V_T$  indicates the Total volume of the solid cube. As per literature review, the infill density of the structure goes on increase, ultimately the porosity of the structure decreases having small pore size & lesser cellular interconnectivity. Aim of this study is to achieve balance between the porosity & infill density of structure to get optimized geometry dimensions.

Required material is first liquefy then placed on a build plate. By using a 3-axis motion, the nozzle can be moved in the XY plane, prints a layer of prototype part. When this layer is completed, the build plate is shifted down one step in Z-direction & that cycle is repeated for next layer until the complete model has been made [1].

In FDM, required material is melted and deposited layer by layer on build plate. By using a 3-axis motion of 3-Dimensional printer, the nozzle is shifted in the X-Y plane which prints a coating of that

model. When this layer is completed, build plate is shifted down to one step in Z-direction & that cycle is repeated for the next layer until the prototype is finalized [1].

Additive manufactured (AM) cellular structures have gained a lot of research attention because of their energy absorption & specific strength capabilities & range of geometric, processing parameters, material highly affect their physical manufacturability & mechanical performance [2].

3D Printing is the technology that is used to convert 3D CAD models to a prototype model [1]. Manufactured cellular structures achieved much research attentiveness because of its strength abilities, range of geometry, material and input processing parameters that affect their manufacturability & mechanical performance [2].

Additive manufacturing has capability to fabricate such triply periodic minimal surface structures because of its built-in manufacturing freedom & layer-by-layer construction. Triply Periodic Minimal Surfaces are non-intersecting 3D surface that are identified by a zero value of mean curvature at every point. The manufacturing orientation in AM has a determining effect that results a good mechanical properties [4].

Scaffolds have potential to provide multi-functional output. Hollow patterns combine mechanical characteristics for different architectures to a unique scaffold [7]. Fused Deposition Modeling model is affected by different process product parameters, whose setting can exert strong impact on respective part strength [8]. By using DOE approach, process-product parameters of FDM like raster angle, bead width, extrusion temperature, air gap, unit cell size, color of part were examined in [9].

FDM is fast-growing Rapid Prototyping technology because it has capability to built models that contains complicated geometrical structure in a very short time interval [10]. Taguchi technique is widely used to optimize process design & product design parameters based on compressive strength investigations [11].

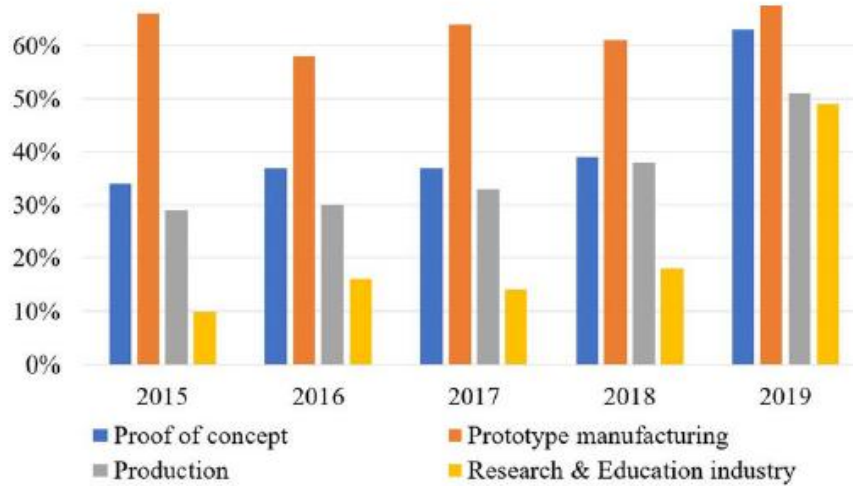


**Figure 2-2:** Division of Additive Manufacturing from 2015 to 2019 in prototype manufacturing, educational industry, production & research [21]

As per figure 2-2, we can see 3D printing technology have become most famous in previous years as it has potential to make fabricate complex geometries which are light in weight, therefore a lot of industries are widely using 3D printing technology which has shown below.

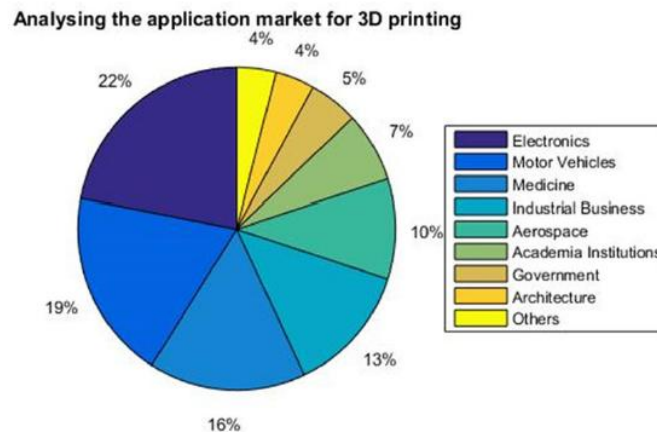


**Figure 2-3:** Main uses of additive manufacturing (AM) technologies in different industries [21]

In figure 2-3, it can be seen different applications of additive manufacturing. A scaffold must having properties of interconnectivity, porosity, pore volume, permeability & other mechanical properties, that make its design, characterization & manufacturing a complex process [23].

Practically & numerically explored deformation mechanisms of AM gyroid, nevius & primitive lattice structures fabricated is studied in [29] by using selective laser sintering (SLS). It can be seen that effect of deformation is more in the bottom of layers than in the upper layers. Higher stacking section lengths results large deformations. When the chamber temperature increases, the deformation will decrease & becomes zero when the chamber temperature becomes equal with

glass transition temperature of material. This is why; it is recommended that material which is used for the part fabrication must have lower glass transition temperature & linear shrinkage rate.

There are different types of scaffold structures which include primitive scaffold structure, neovius scaffold structure, diamond scaffold structure and gyroid scaffold structure. The primitive scaffold gained the best output in compression at 90 degree [4]. Strength increases with increase in thickness and no. of cells [2]. 90 degree & negative air gap enhances tensile strength [1]. Specimens which are filled with the honeycomb patterns are stiffer and stronger as compared with rectangular pattern structures [12]. The PLA has better thermo mechanical properties than ABS material that have a strong mechanical resistance property & preferred angle is 45 degree [13]. The specimens which are fabricated with 0 degree orientation has the highest Young's modulus, for tensile test [14].

Tensile Strength increases as increase in raster angle & layer thickness [10]. For minimum number of layers, smaller raster lengths is suggested [10]. Primitive Surface shows the highest mechanical properties among Gyroid & Diamond Structure [23]. Neovius possess higher stiffness & strength than primitive structure [3].

Smallest unit cell has highest strength & highest volume fraction [15]. Strength increases as increase in no. on contours [8]. When layer thickness increases, it increases the tensile strength, ductility & yield strength of material [16]. Increase in printing temperature enhances mechanical strength of part [17]. Increase in layer thickness reduces printing time [18]. Tensile strength enhances with the infill density up to 40%, after this limit its decrease with increase in infill density [19].

The research has shown that increase in infill density enhances the mechanical strength as input parameter fabricates the part more solid & decreases number of cavities. Increase in layer height maximizes tensile strength [31].

Short raster length & 0-degree orientation is suggested in [10] to achieve best tensile strength. Surface roughness increase as increase in layer thickness & decrease in orientation angle. Air gap & width do not affect surface finish [20]. High infill density & high extrusion width yields maximum compressive strength for gyroid [21].

## **2.4. 3D Printing CAD Interface**

Main step in printing 3D objects involve the selection of suitable CAD software. First step is to convert 3D model design into suitable rapid prototyping format which is STL format widely used. Different formats can be seen in table 2-1. Few widely used CAD software are Pro-E, Solidworks, 3DS MAX, CATIA, Blender, AUTOCAD, Fusion 360. They have capability to store the designed model in form of mathematical data which can be transmitted using the standardized formats i.e. STL, STEP, IGES, DXF etc. Most of the rapid prototyping use STL format that works as input to slicing software which then slices the model into layers to fabrication.

**Table 2-1:** Available standard formats for rapid prototyping [21]

Interfaces available today	Full Form
IGES	Initial Graphic Exchange Specification
STEP	Standard for Exchange of Product data
DXF	Drawing Exchange format
STL	Standard Tessellation Language

## 2.5. Fused Deposition Modeling (FDM)

FDM is an additive manufacturing technique that fabricates the material by layer upon layer coating of extruded materials usually polymers. In FDM, 3D CAD model of structure is designed firstly & then it is converted to the stereo lithography (STL) file format. Then STL file is checked for any kind of defects such as mesh defects, missing faces etc before the structure is sent for the slicing operation. The build process and time to fabricate depends upon the geometry's complexity. The printing nozzle's motion is controlled by a motor, which deposits layer of desired material at very high temperature so that material's adhesiveness increases which then solidifies rapidly. A schematic diagram of FDM process can be seen in figure 2-4.

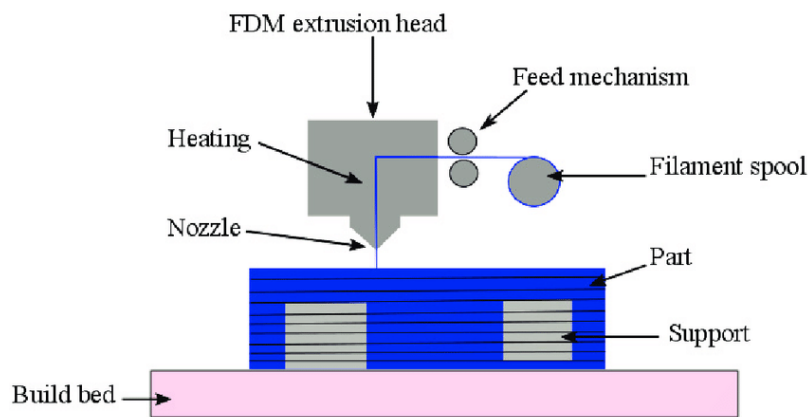


**Figure 2-4:** FDM process schematic diagram [25]

FDM is a low processing cost, less contamination of working material, low wastage of material, easily operated & works as user friendly environment. But at the same time there are some disadvantages linked with the FDM process such as longer build time with lower material strength, less dimensional accuracy, deposition of residual material within the layers etc. The cost of manufacturing and build time highly depends upon selection of FDM process-product parameters. Therefore, process-product parameters must be kept in mind while fabricating the material.

## **2.6. FDM Process Parameters**

FDM process-product parameters exert a key role in determining the strength of 3D printed scaffold structures. Different number of process-product parameters is shown in figure 2-5. Better surface quality, low cost, dimensional accuracy, best strength can only be achieved by selecting suitable process product parameters. Therefore, It is important to explore the effect of various process-product parameters & also how did they affect the structure. Therefore, study of the relevant parameters is compulsory to get good results. Most common process-product parameters in literature are described below:

### **2.6.1. Orientation:**

Part build orientation cite to inclination of object in a build plate with respect to the X, Y & Z axis, where X & Y-axis are considered to be in parallel position to the build plate & Z-axis is along direction of part build.

### **2.6.2. Layer thickness:**

It is a thickness of layer of melted material which is deposited by the nozzle and it depends on type of nozzle used.

### **2.6.3. Raster angle:**

Raster angle is the direction of raster relative to X-axis of build plate.

### **2.6.4. Part raster width:**

Width of raster pattern used to fill internal regions of object.

### **2.6.5. Raster to raster gap:**

This is the gap between two adjacent rasters on the same layer.

### **2.6.6. Extrusion Temperature:**

Temperature at which material is melted in heater to fabricate part by layer upon layer.

### **2.6.7. Unit cell size:**

Scaffold structure comprises of different unit cells. These cells may be identical or may not be.

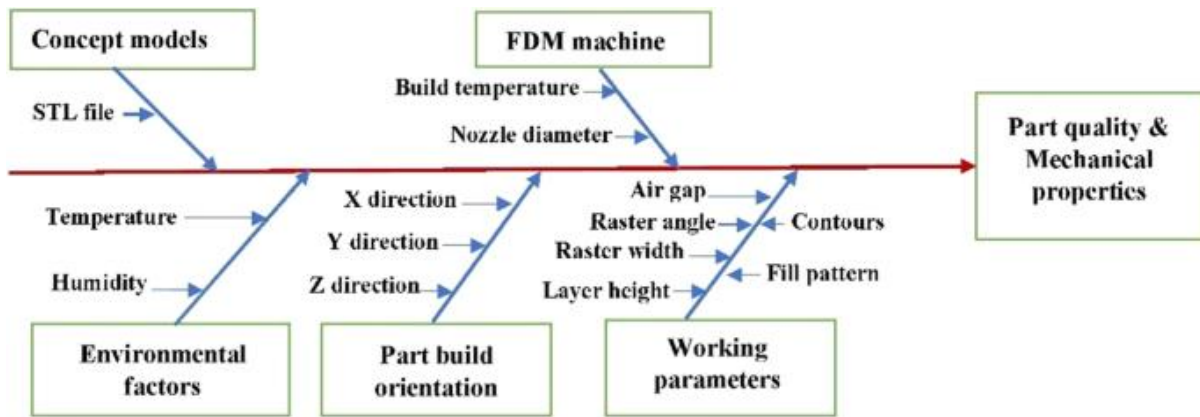


Figure 2-5: Input parameters that are influencing strength of structure

## 2.7. 3D Printed Cellular Structures for Tissue Engineering

3D printed cellular structures are typically designed for biomedical engineering applications in order to provide support structures for defective organs in the body. Scaffolds are temporary support structures that aid in tissue growth on defective or damaged bones in body. Design of scaffolds with best mechanical properties is essential for tissue regeneration and function to restore.

A new generation of printed 3D scaffolds will work after the upgrade understanding the effect of bio-physical and bio-chemical signals on cell behavior. The strength of 3D scaffolding plays a very important role in resisting compressive force bone behavior especially when scaffolds are used for bone grafting and the effect of the various FDM parameters in the 3D scaffolding machine provide extensive research a place for future studies. Scaffolds used in tissue regeneration. Various methods used on tissues engineering.

The main function of the scaffold is to direct the development of new tissues through surgery cellular interaction, mechanical stability, blood circulation and waste disposal from a paralyzed part of the body as shown in figure 2-6. Compressive strength highly depends on geometry of scaffold structures. Porosity of structure is the amount of empty space available in a solid area. Scaffold structures with high porosity and with the help of a suitable hole size for skeletal muscles to grow well, However by increasing porosity weight of structure can also be reduced.



## Bone tissue engineering

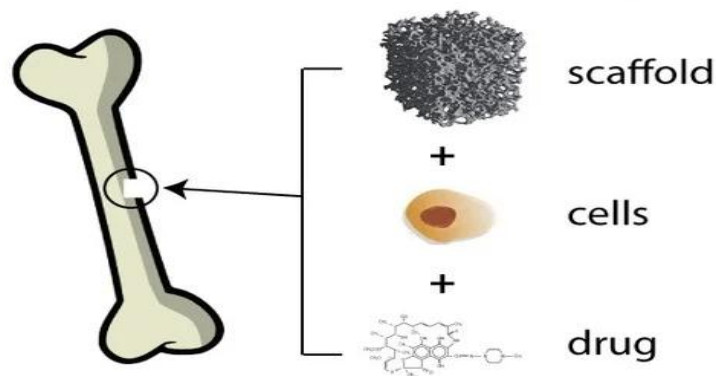


**Figure 2-6:** Repair of bone defects using bone tissue engineering scaffolds [26]

A very short work is there on internet on the output of FDM process-product parameters on strength of 3D printed primitive scaffold structure. Complex geometry scaffold structures can easily be fabricated using 3D printing. Mechanical strength of structure highly depends upon the porosity and infill density of scaffold structure. The scaffolds used in biomedical engineering must have following properties:

- Scaffold should promote better cell attachment so that tissues transmission and growth can be done easily.
- Scaffolds must possess better bioactivity to help cellular migration attached within the structure through blood flow.
- Scaffold must be non-toxic.
- Best cellular interaction with each other makes the scaffolds good in tissue engineering technology.
- Scaffold structures must have better mechanical properties to tolerate the flexural, compressive, tensile loads within the body.
- Must have ease of processing and fabrication. Scaffold should have better porosity for ease of access to defected area for tissues or cells.

### 2.8. Research Gap and Challenges

Following are the main findings of this study:

- Mostly study on this topic has been done by considering only one process parameter or one material property. In order to achieve good performance and results, several process product parameters and material properties should be considered during rapid prototyping.
- From previous studies, it is clear that to improve material properties, different process product parameters should be thoroughly studied as each value of that particular parameter have

specific influence on material's strength As per literature review, The primitive scaffold gained the best output in compression at 90 degree [4]. Strength increases with increase in thickness and no. of cells [2] 90 degree & negative air gap enhances tensile strength [1] Specimens that are filled with honeycomb patterns are more stronger than those patterns which are rectangular [12] The PLA posses better thermo mechanical characteristics than ABS having a stronger mechanical resistance & suggested angle is 45 degree [13] 0<sup>0</sup> printing orientation has the highest Young's modulus as output, for tensile test [14].

- As there is little study done on 3D printing and on FDM process product parameters, there need for a lot of study to be done in this particular area as fabrication time also highly influence the mechanical strength of structure.
- There need to study different process product parameters by using Taguchi Design of Experiments (DOE) technique.
- Normally PLA or ABS is used in most of the study. As material strength highly depends of material's properties therefore new hybrid material must be introduced which may highly influence the properties of scaffolds.
- Based on the literature review, we have chooses those process product parameters in this study that must have very crucial effect on mechanical strength of 3D printed scaffolds. Those parameters include layer thickness, raster angle and unit cell size & extrusion temperature.
- Studied the combined effect of extrusion temperature, layer thickness, raster angle, unit cell size on compressive strength of 3D printed scaffolds on UTM unlike previous studies that only dealt with one or two FDM process or product parameters.

## CHAPTER 3: MATERIALS AND METHODS

### 3.1. Methodology

Methodology in this work is carrying out as per the flow chart shown in table 3-1. First step is to make geometric design in CAD software. For this purpose CREO parametric 7.0 versions is used in which 27 samples are designed. In 2<sup>nd</sup> step which is design of experiment, Taguchi analysis is done in minitab. Taguchi suggested experimental plan in terms of orthogonal array which gives out different combinations of parameters and their levels for the each experiment. In 3<sup>rd</sup> step which is 3D printing, those 27 CAD files are fabricated on 3D printer by using 2 size nozzles i.e, 0.2 mm & 0.3 mm. in 4<sup>th</sup> step which is strength test, those 27 samples are tested for compression on UTM at 50 KN load. In 5<sup>th</sup> step which is analysis of variance, regression analysis is done in minitab in which design parameters are ranked on their S/N ratio. In 6<sup>th</sup> step, we got stress, strain and maximum force values from UTM test and arranged in a table. In 7<sup>th</sup> step which is validation of result, a new 28<sup>th</sup> part has been fabricated after ANOVA results from 27 parts and its strength was high as compared with the remaining 27 samples.

**Table 3-1:** Flowchart of methodology

Sequence	Steps	Briefing
1	Geometric Design	Unit cell design using CAD software (Creo Parametric 7.0).
2	DOE	<ul style="list-style-type: none"> <li>• Used Taguchi L<sub>27</sub> array.</li> <li>• Raster angle, Unit cell size layer thickness and extrusion temperature is used as design parameters.</li> </ul>
3	3D Printing	<ul style="list-style-type: none"> <li>• Creality CR-10 Pro is used for 3D printing.</li> <li>• Nozzle diameter 0.2, 0.3 mm is taken.</li> </ul>
4	Strength test	<ul style="list-style-type: none"> <li>• Compression tests are performed to check strength.</li> <li>• Load of 50 KN is used at 2.9 mm/min.</li> </ul>
5	ANOVA	<ul style="list-style-type: none"> <li>• Regression analysis is done.</li> <li>• Design parameters are ranked on their S/N ratio.</li> </ul>
6	Results	<ul style="list-style-type: none"> <li>• Stress &amp; maximum force is considered.</li> <li>• ANOVA results suggest the optimal design parameters combinations for maximizing strength.</li> </ul>
7	Validation of result	A part has been manufactured on the best suited parameters got from ANOVA results and their strength has been tested and compared with the other 27 parts.

Taguchi technique is widely used to optimize process design & product design based on compressive experimental investigations [11]. Taguchi Design of Experiment (DOE)  $L_{27}$  array has been used in this work for performing number. of experiments with four different process-parameters such as , layer thickness, raster angle, unit cell size & extrusion temperature having three level of input values.

## 3.2. Selection of Input Parameters

### 3.2.1. Raster Angle

Raster angle is angle between nozzle path & X-axis of build platform while 3D printing of samples as shown in figure 3-1. Normally raster angle could be changed from  $0^{\circ}$  to  $90^{\circ}$ . Raster angle has a great effect on mechanical strength especially on compressive strength & tensile strength of 3D printed materials [10]. In one study, it is very clear that by changing the raster angle build cost, build time and amount of material being used is highly influenced. Tensile Strength increases as increase in raster angle [10]. Different number of raster angles are used are shown in Figure 9.

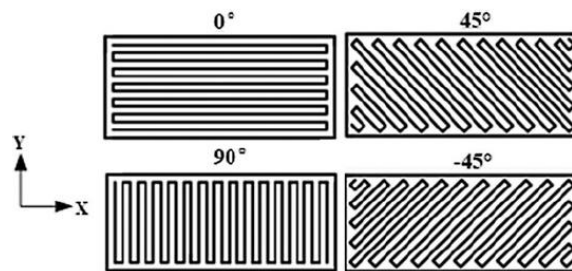


Figure 3-1: Different raster angles

### 3.2.2. Unit Cell Size

Unit cell size is applied to control the infill density of part as small size of unit cell gives higher infill density (%) if compared with larger unit cell sizes. In [15], effect of unit cell sizes with volume fractions is investigated. The output was that the unit cell sizes ranges from 2-8 mm say (2, 3.5, 4.5, 5.5, 6.5, and 8 mm), where volume fraction of 15% is used to fabricate lattice of  $25 \times 25 \times 15 \text{ mm}^3$  dimension without any defects and obviously without using any supporting materials while fabricating the parts. Unit cell size's effect on infill density of solid structure & compressive strength is also judged and as per results, using smaller unit cell size, density goes on increases while increase in unit cell size decrease mechanical strength.

### 3.2.3. Layer Thickness

Layer thickness can be defined as the width of one extruded filament which is deposited while fabricating of materials or parts & it is a measure of layer's height as shown in figure 3-2. In one study [41], it was found that smaller extrusion widths are among the optimal parameters while investigating the the effect of layer thickness on strength.

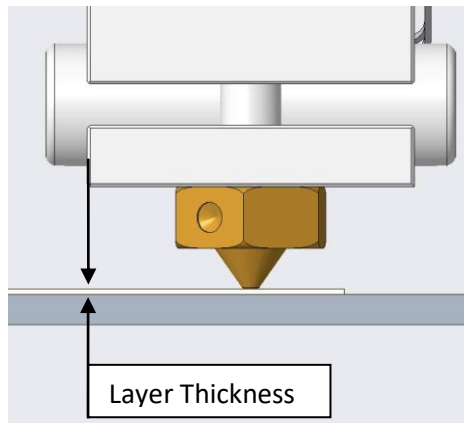


**Figure 3-2:** Representation of extrusion width or layer thickness [28]

Strength increases layer thickness enhances [2]. Tensile Strength also increases with enhancement in layer thickness [10]. Maximum numbers of layer enhances the entire mechanical properties of the part [10]. The increase in layer thickness enhances the yield strength, tensile strength, ductility [16]. But there is a disadvantage of increasing the layer thickness is that surface roughness increases with increase in layer thickness [20]. Even fabrication cost also increases as layer thickness increases.

#### **3.2.4. Extrusion Temperature**

The main parameter that is meant to control is the temperature fluctuations because large fluctuations in temperature can obviously exert negative effects while a print up. Warping occurs when printed layers are cooling down rapidly. Higher extrusion temperature needs time to melt layers quickly. Normally a temperature of 220° C is used for ABS & for PLA normally at speeds of 40 mm/s and lower while 230° C extrusion temperature at speed normally up to about 100 mm/s. [9] investigated the effect of temperature on fabrication of parts while print up. Increase in printing temperature enhances mechanical strength of part [17]. In our study, three levels of temperatures are considered which includes extrusion temperature of 200<sup>0</sup>C, 210<sup>0</sup>C, 220<sup>0</sup>C.

The factors with their levels of input are given in Table 3-2:

**Table 3-2:** Varying values of FDM input process-product parameters

<b>Parameters</b>	<b>Level 1</b>	<b>Level 2</b>	<b>Level 3</b>	<b>Units</b>
<b>Unit Cell Size</b>	6	8	10	mm
<b>Raster Angle</b>	15	30	45	Degree
<b>Layer thickness</b>	0.2	0.25	0.3	mm
<b>Extrusion Temperature</b>	200	210	220	Degree Centigrade

Based on these variables as FDM parameters, different numbers of combination were made with using Taguchi  $L_{27}$  orthogonal array (OA). Total 27 different combinations were made using orthogonal array which shown in Table 3-3. Different combinations were made by using Minitab 2017 software which has generated combinations on randomly to reduce the noise factor to minimum level. Those 27 samples are then fabricated on 3D printer for compression test. Taguchi  $L_{27}$  orthogonal array (OA) is shown in Table 3.-3.

**Table 3-3:** Taguchi  $L_{27}$  Orthogonal Array (OA) table

Sample Number	Raster Angle	Unit Cell Size	Layer Thickness	Printing Temperature
	Degree	mm	mm	Degree Centigrade
1	15	6	0.2	200
2	15	6	0.2	210
3	15	6	0.2	220
4	15	8	0.3	200
5	15	8	0.3	210
6	15	8	0.3	220
7	15	10	0.25	200
8	15	10	0.25	210
9	15	10	0.25	220
10	30	6	0.3	200
11	30	6	0.3	210
12	30	6	0.3	220
13	30	8	0.25	200
14	30	8	0.25	210
15	30	8	0.25	220
16	30	10	0.3	200
17	30	10	0.3	210
18	30	10	0.3	220
19	45	6	0.25	200
20	45	6	0.25	210
21	45	6	0.25	220
22	45	8	0.2	200
23	45	8	0.2	210
24	45	8	0.2	220
25	45	10	0.3	200
26	45	10	0.3	210
27	45	10	0.3	220

### 3.3. Fabrication of Samples

All samples were fabricated as per Table 3-3 for compression testing. Samples are fabricated on 3D printer creality CR-10 pro, which is an additive manufacturing technology for 3D printing. The machine setup for 3D printing is shown in Figure 3-3.

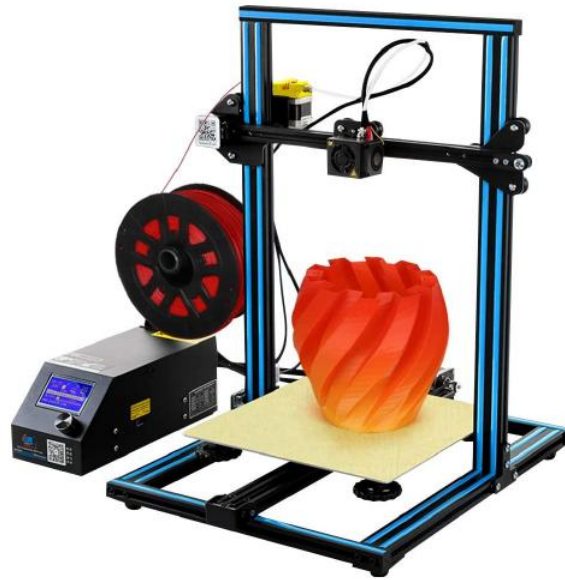


**Figure 3-3:** 3D printing "Creality CR-10 Pro" machine setup

Materials such as PLA, PEEK, PC, ABS etc are used to fabricate in this machine in order to print the part with customized setting and accuracy.

The 3D CAD models of primitive scaffold structure with nine different unit cells and layer thickness are designed on Creo Parametric 7.0 version in order to achieve the required infill densities & then these are converted to STL files for 3D printing of the specimens. The dimensions of models are according to ASTM D695-15. The STL files are sent to the slicing software where we can also select input process parameters which are layer thickness, raster angle & unit cell size according to experimental plan yielded from Taguchi Design of Experiment (DOE) by using minitab 2017. The STL files design of 3D CAD models of nine geometries by using three different unit cell sizes & layer thickness for achieving different infill densities. Few of them are shown Figure 3-4.

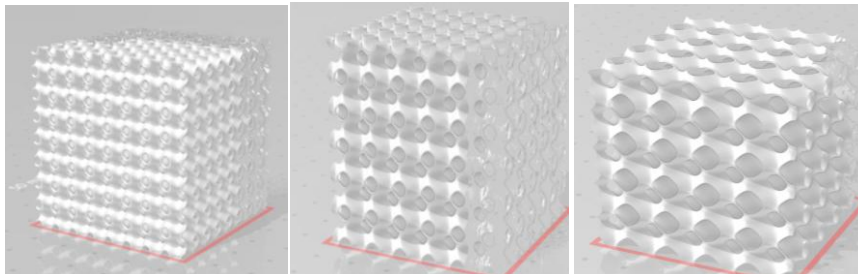


**Figure 3-4:** CAD models of primitive scaffold structures

PLA was inserted into the 3D printing machine in form of spool. A Specific kind of wheel is used for purpose of handling and pushes the material from spool to 3D printing machine. Material is first

heated above its solidification temperature & then extruded using of set of nozzles. One is used for the extruding working material while the other nozzle is then used for the extrusion of supporting the material. First layer of PLA is extruded at very high temperature than remaining layers in order for achieving best adhesion of layers. There were some fixed process parameters which are given below in table 3-4:

**Table 3-4:** Fixed FDM parameters of 3D printer

<b>Fixed FDM parameters</b>	
3D printing machine	Crealty CR-10 PRO
Material	PLA
Bed Temperature	85 <sup>0</sup> C
Layer thickness	0.2 mm, 0.25 mm, 0.3 mm
Infill Density	100%
Print Speed	2700 mm\min
Slicing software	Simplify 3D
Nozzle Diameter	0.2 mm, 0.3 mm

The input parameters which are Layer thickness, Raster Angle, Unit Cell Size & Extrusion Temperature are used with three different levels as input as mentioned in Table 3-2, by using Taguchi L27 orthogonal array (OA) total of 27 different combination are made to fabricate 27 samples as per ASTM D695-15. Compression tests are done to judge mechanical strength under loading conditions. Twenty seven parts for compression tests were manufactured by using the data given in Table 3-3. Out of 27 samples, pictures of 9 samples are shown in Figure 3-5.



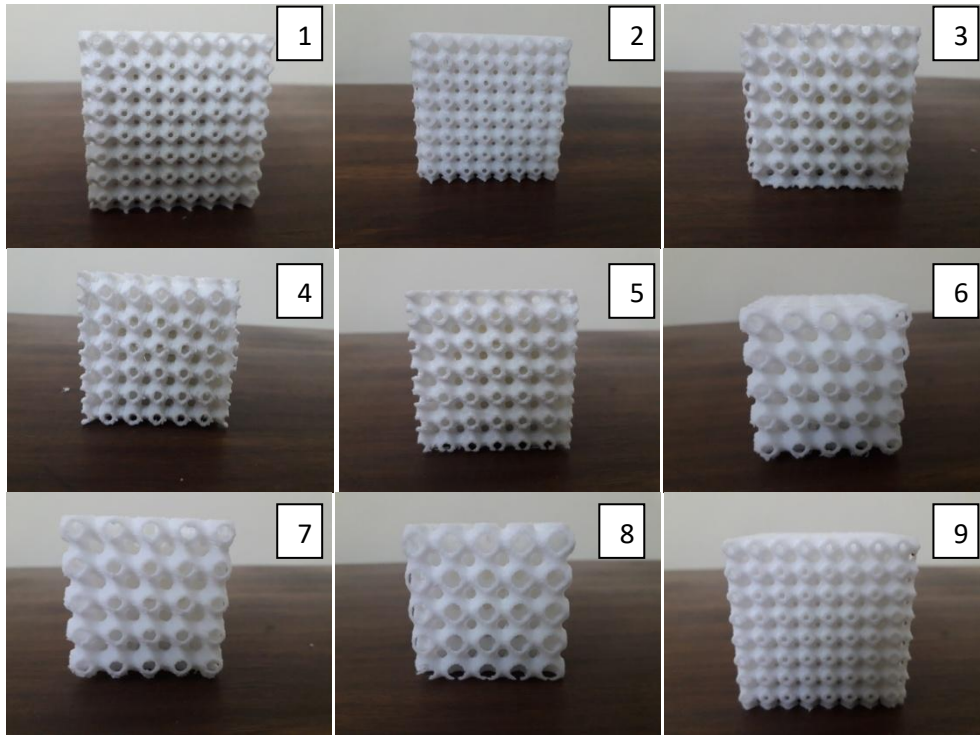


**Figure 3-5:** 3D printed primitive scaffold 9 samples

The infill density (%) can be controlled by unit cell size as there is a wall thickness present for this design geometry. Infill density of the structure having different unit cell sizes is below.

$$\% \text{Infill} = m/m_s \quad (3)$$

where,  $m$  represents Actual mass of cube &  $m_s$  represents mass of solid cube.

Requirements for compression tests & tests settings are described in the next subsection for entire 27 samples to judge their mechanical strength.

### **3.4. Compression Testing Requirements and Specifications**

The parts which are subjected for compression tests are prepared as per ASTM D695-15 standard method for cellular rigid plastics for compression testing. A picture after compression test is shown in figure 3-6. The tests yields with the maximum yield stress, maximum break force, break stress, break strain, maximum load at fracture and deflection at maximum stress. The samples are prepared as per ASTM D695-15 which is a standard test method to test compressive properties of rigid plastics in cylindrical or cube shape.

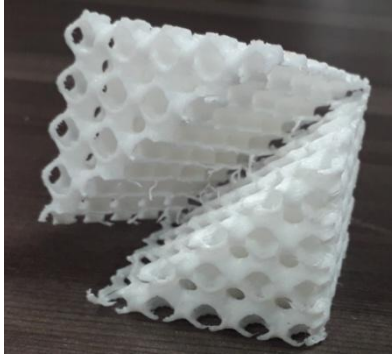


**Figure 3-6:** Sample subjected to compression test

The dimensions of parts which are fabricated in our study were described as cube of 48 mm in length, width & height of primitive structure. The tests are carried out on Universal Testing Machine (UTM) with crosshead speed of 2.9 mm/min and load of 50 KN.

## CHAPTER 4: RESULTS AND DISCUSSION

To print 3D samples for compression tests according to ASTM D695, Taguchi  $L_{27}$  orthogonal array (OA) results are used. This study yields information regarding overall influence of this Layer thickness, extrusion temperature, raster angle and unit cell size. Compression tests are performed randomly in to avoid any experimental biased results.

### 4.1. Compression Tests Specimens

Compression tests were done on the samples that were fabricated using nozzle diameter 0.2 mm & 0.3 mm. Parts having layer thickness 0.25 were made by controlling the feed rate of 3D printer. Unit cell size was taken as a input parameter in our study as very little information is available from previous work in this field regarding impact of unit cell size on the mechanical strength of the samples fabricated by rapid prototyping. There were also some inconsistencies on impact of the layer thickness on the mechanical strength, but in our study, the result we gained is maximum the layer thickness, higher compressive strength will be, as compared to the smaller layer thickness.

**Table 4-1:** Compression tests of all samples on UTM

Part Number	Raster Angle	Unit Cell Size	Layer Thickness	Printing Temperature	Max Force
	Degree	mm	mm	Degree Centigrade	N
1	15	6	0.2	200	4400.56
2	15	6	0.2	210	3926
3	15	6	0.2	220	8190
4	15	8	0.3	200	4326.71
5	15	8	0.3	210	2951.70
6	15	8	0.3	220	3026.69
7	15	10	0.25	200	2631.58
8	15	10	0.25	210	2697.39
9	15	10	0.25	220	2558.58
10	30	6	0.3	200	7426.95
11	30	6	0.3	210	7957.36
12	30	6	0.3	220	8031
13	30	8	0.25	200	3210.73
14	30	8	0.25	210	3034.43
15	30	8	0.25	220	2141.07
16	30	10	0.3	200	2114.82
17	30	10	0.3	210	2630.79
18	30	10	0.3	220	1466.41
19	45	6	0.25	200	8881.31
20	45	6	0.25	210	8879.74
21	45	6	0.25	220	7845.08

22	45	8	0.2	200	3420.21
23	45	8	0.2	210	3307.83
24	45	8	0.2	220	3074.29
25	45	10	0.3	200	2797.91
26	45	10	0.3	210	1770.12
27	45	10	0.3	220	2085.06

The stress of all fabricated samples can be seen in Table 4-2. The results showed the maximum compressive strength for the samples fabricated at higher value of layer thickness & at higher infill density. 50 KN of load was applied on the samples till their yield point. The maximum force of all fabricated samples can be seen in table 4-1. The regression analysis was carried out on Minitab 2017 software to identify simultaneous impact onto compressive strength of each parameter. Stress was calculated as per equation (4).

$$Stress = Force / Area \quad (4)$$

area of structure is the minimum total area. The formula by using which minimum total area is calculated is given in equation (5)

$$Minimum\ total\ area = number\ of\ cells * Ring\ Area \quad (5)$$

where, ring area is difference between outer area and inner area.

As per figure 4-1, one can easily compare the results of entire parts. Overall six parts has shown good properties among remaining 27 parts which include p10, p11, p12, p19, p20, p21. Those parts can bear stress having value more than 3 Mpa while there are four parts, p3, p12, p19, p20 which can bear stress upto 40 Mpa.

**Table 4-2:** Stress test for all samples done on UTM

Part number	Raster Angle	Unit Cell Size	Layer Thickness	Printing Temperature	Stress
	Degree	mm	mm	Degree Centigrade	MPA
1	15	6	0.2	200	37.22
2	15	6	0.2	210	33.21
3	15	6	0.2	220	34.82
4	15	8	0.3	200	32.7
5	15	8	0.3	210	22.31
6	15	8	0.3	220	21.8
7	15	10	0.25	200	27.3
8	15	10	0.25	210	27.98
9	15	10	0.25	220	37.19
10	30	6	0.3	200	42.17
11	30	6	0.3	210	45.18

12	30	6	0.3	220	40.86
13	30	8	0.25	200	29.04
14	30	8	0.25	210	27.45
15	30	8	0.25	220	18.3
16	30	10	0.3	200	18.32
17	30	10	0.3	210	22.79
18	30	10	0.3	220	25.49
19	45	6	0.25	200	60.3
20	45	6	0.25	210	60.29
21	45	6	0.25	220	49.77
22	45	8	0.2	200	38.57
23	45	8	0.2	210	37.31
24	45	8	0.2	220	18.49
25	45	10	0.3	200	24.23
26	45	10	0.3	210	15.33
27	45	10	0.3	220	30.31

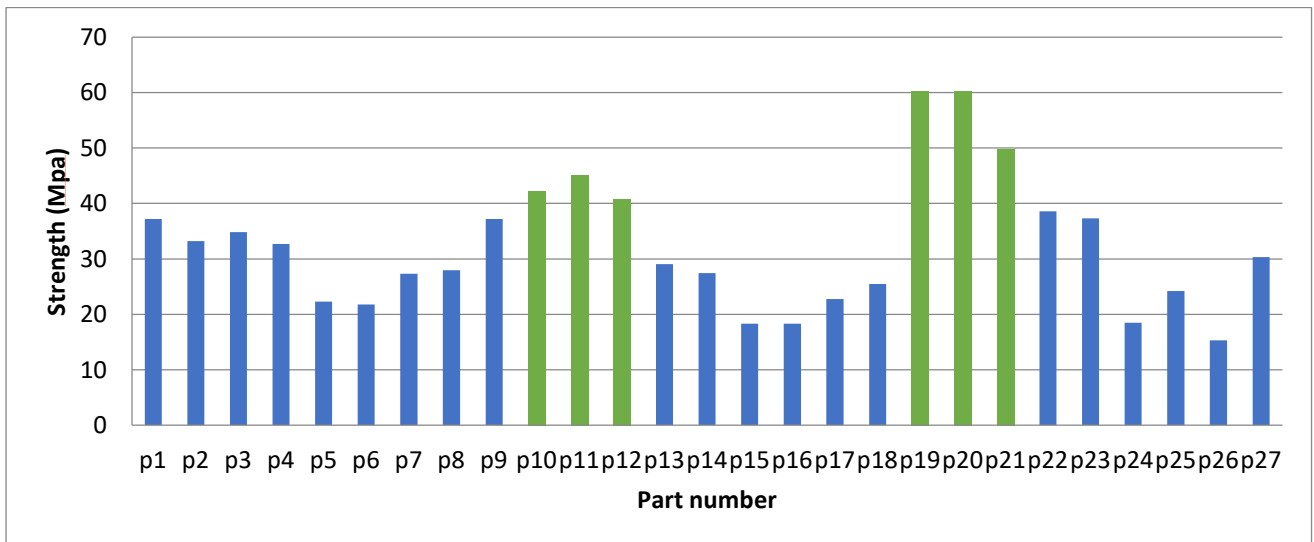


Figure 4-1: Strength graph of 27 samples

## 4.2. Statistical Analysis

### 4.2.1. Regression Analysis

The linear regression analysis was carried out in Minitab 2019 software to find out the simultaneous parametric that effect the compressive strength. The effect of each parameter is explained by P-value i.e. the critical P-value for significance is about 0.05 which is threshold of significance. The data shown in table 4-3 is taken from Minitab 2019 software which describes the P-values for input parameters. The P-value for layer thickness is very close to critical value. This suggests that impact of layer thickness lies on borderline of significance.

**Table 4-3:** P value

Analysis of Variance for Means						
Source	DF	Seq SS	Adj SS	Adj MS	F	P
Raster Angle	2	3013402	4346381	2173191	1.95	0.171
Unit Cell Size	2	127330848	131915861	65957930	59.25	0.000
Layer Thickness	2	7890262	7890262	3945131	3.54	0.050
Extrusion Temperature	2	238803	238803	119401	0.11	0.899
Residual Error	18	20036591	20036591	1113144		
Total	26	158509905				

Model Summary		
S	R-Sq	R-Sq(adj)
2.0848	86.26 %	80.16 %

The “Larger is Better” approach is utilized for the fact to maximize impact factor on mechanical strength. The main influence of plots in FDM input parameters for the compressive strength according to “Larger is Better” approach using Minitab 2017 software can be seen in figure 4-2.

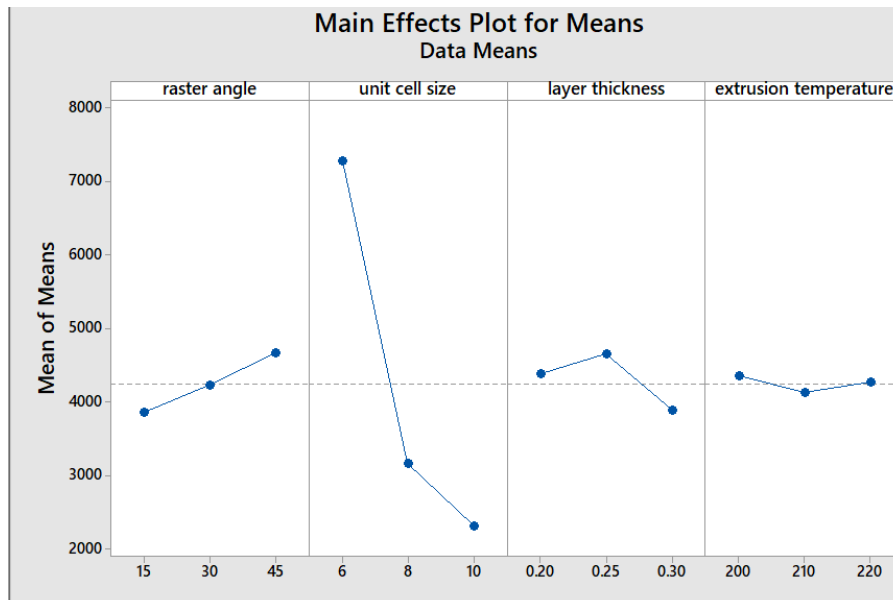


**Figure 4-2:** Main impact plots for compressive strength

“Signal to Noise” ratio approach is used to maximize response variable and to reduce the variability of noise in response variable as shown in figure 4-3.

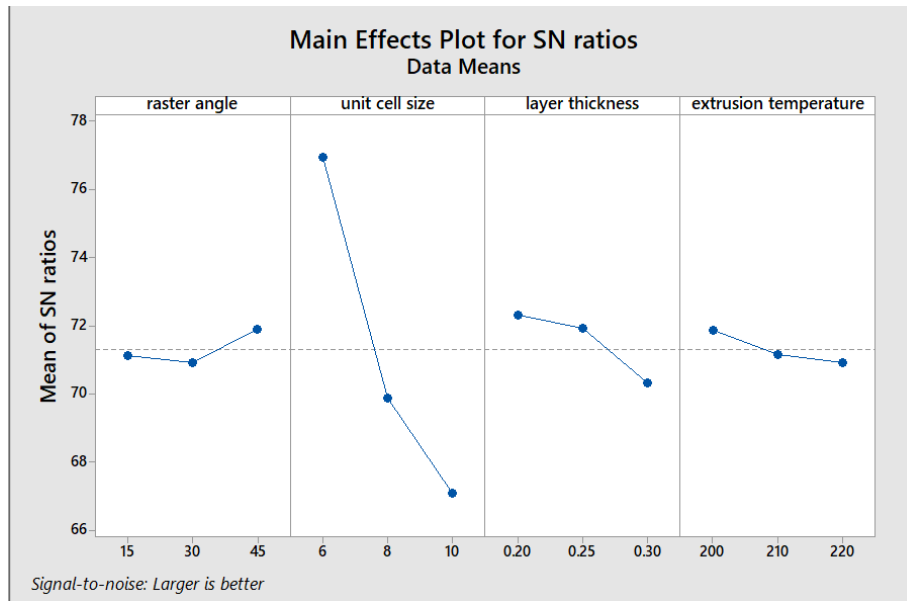


**Figure 4-3:** Main effect plot for means and S/N ratio

However, the interaction between the input factors also suggests that the process parameters are not completely independent. The regression equation for maximum compressive strength with R-Sq value of 86.26% is given in equation (6):

$$\sigma_c = -952565 + 37421A + 102798U + 3576636L + 4588T - 4213AU - 138383AL - 178AT - 381361UL - 491UT - 17171LT \quad (6)$$

where, A =Raster Angle, U=Unit cell size, L=Layer thickness. T=Extrusion temperature

The contour plots are plotted to show three dimensional impacts of FDM parameters on two dimensional surface depending upon the interaction between input parameters. Plots were made using Minitab 2019 software for maximum compressive strength taking input parameters unit cell size, raster angle, layer thickness, extrusion temperature and input parameter raster angle VS unit cell size, layer thickness, extrusion temperature. The plots shown in figure 4-4, figure 4-5, figure 4-6, figure 4-7, figure 4-8, figure 4-9 describes impact of two input parameters while holding the constant value for third one.

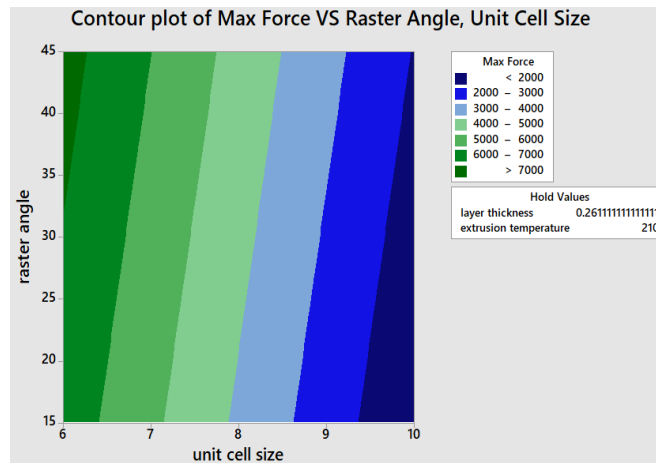


Figure 4-4: Contour plot for max stress VS unit cell size, raster angle

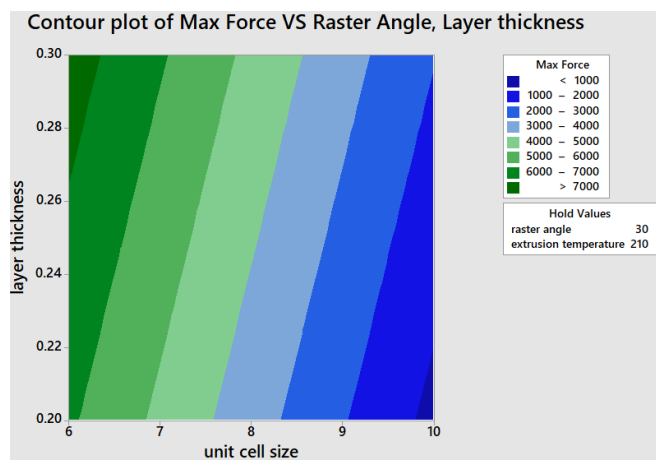


Figure 4-5: Contour plot for max stress VS unit cell size, layer thickness

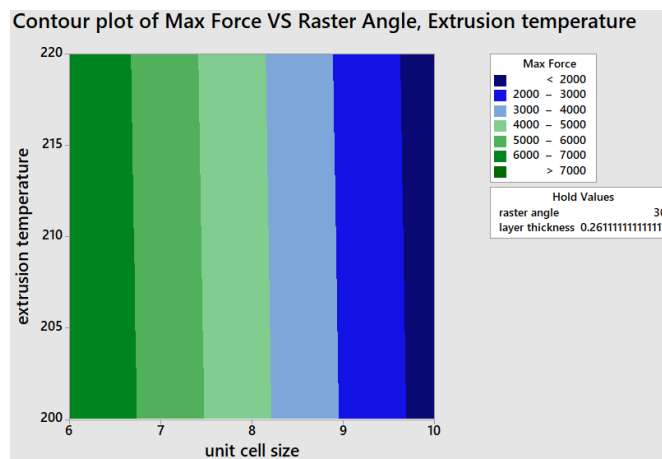


Figure 4-6: Contour plot for max stress vs unit cell size, extrusion temperature



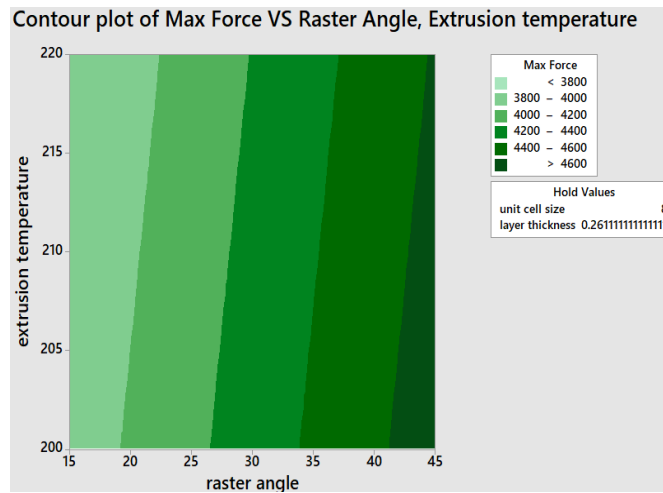


Figure 4-7: Contour plot for max stress vs raster angle, extrusion temperature

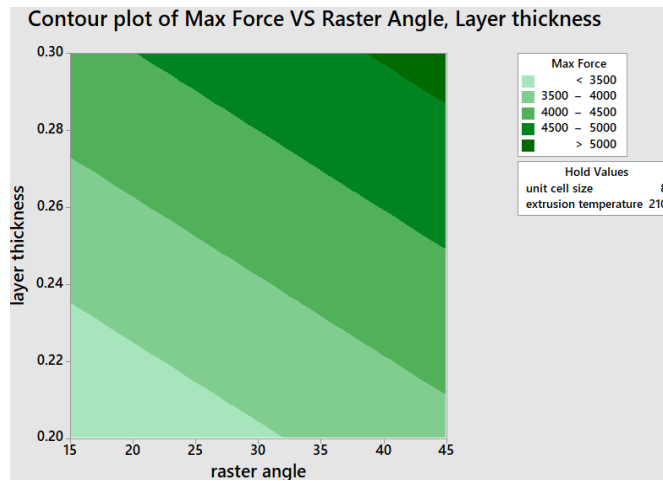


Figure 4-8: Contour plot for max stress VS raster angle, layer thickness

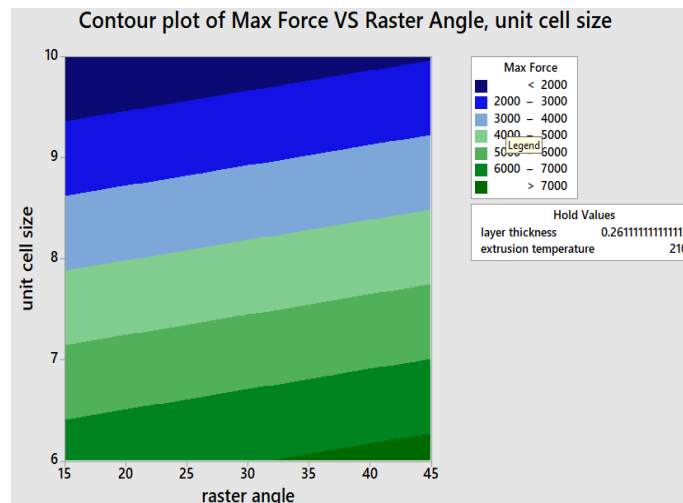


Figure 4-9: Contour plot for max stress VS raster angle, unit cell size

From the contour plots, it can be seen that for holding the fixed value of layer thickness or extrusion width, maximum stress can be obtained for maximum value of raster angle 45 degree and also at higher value for unit cell size of 6 mm.

### 4.3. Results and discussion

The table 4-1 shows the results of 27 models. Maximum force represents the maximum force exerted on the material to deform it then the force began to reduce. Similarly other slots are of stress & strain. Smallest UC size shows the highest strength as compare to UC 8 mm & UC 10 mm. besides, it is clear from the results that maximum value of layer thickness fabricate a more strong part than the part having less layer thickness. Strength increases with increase in thickness and no. of cell. Increase in layer thickness also reduces the printing time.

Another parameter which directly affects the part strength is extrusion temperature. Increase in printing temperature enhances mechanical strength of part. Besides, raster angle has also very important effect on mechanical strength. The more the raster angle, more the strength will be. The main impact plots of FDM input parameters for compressive strength according to “Larger is Better” approach from Minitab 2017 software are shown in Figure. The optimal parameters with their respective levels are found using Minitab software and values appeared are raster angle = 45 degree, unit cell size = 6 mm, layer thickness = 0.3 mm & extrusion temperature= 220<sup>0</sup> C. All the values were obtained using “Larger is Better” approach and the confidence level of 95%.

Based on results of those 27 models, the optimal parameters in this study were obtained for maximum compressive stress by using Minitab 2019 software. The optimal levels are shown in Figure 4-10. The factors which are described in figure 4-10 by Cur in red color are the optimal ones in this study to gain maximum compressive strength.

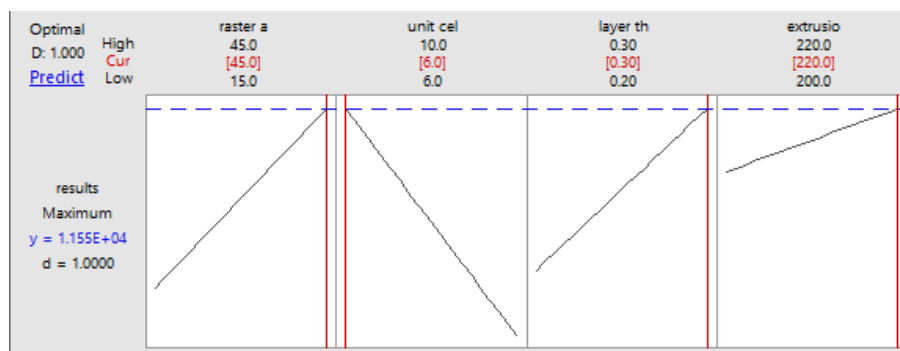
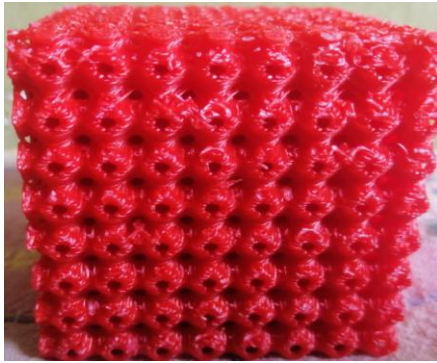


Figure 4-10: Optimal factors values for maximum compressive strength

A new sample part 28 was then fabricated as per those optimal parameters which are shown in figure 4-11. This sample was then tested to achieve its value for stress and to know how much compressive strength it can bear.



**Figure 4-11:** 28th sample having fabricated on base of optimized parameter using ANOVA

It yields much more good result as compared with the other 27 parts. It yields 10550.6 N max forces and max stress is 65.9 Mpa. Result difference between 27 samples and that 28<sup>th</sup> sample can be seen in figure 4-12.

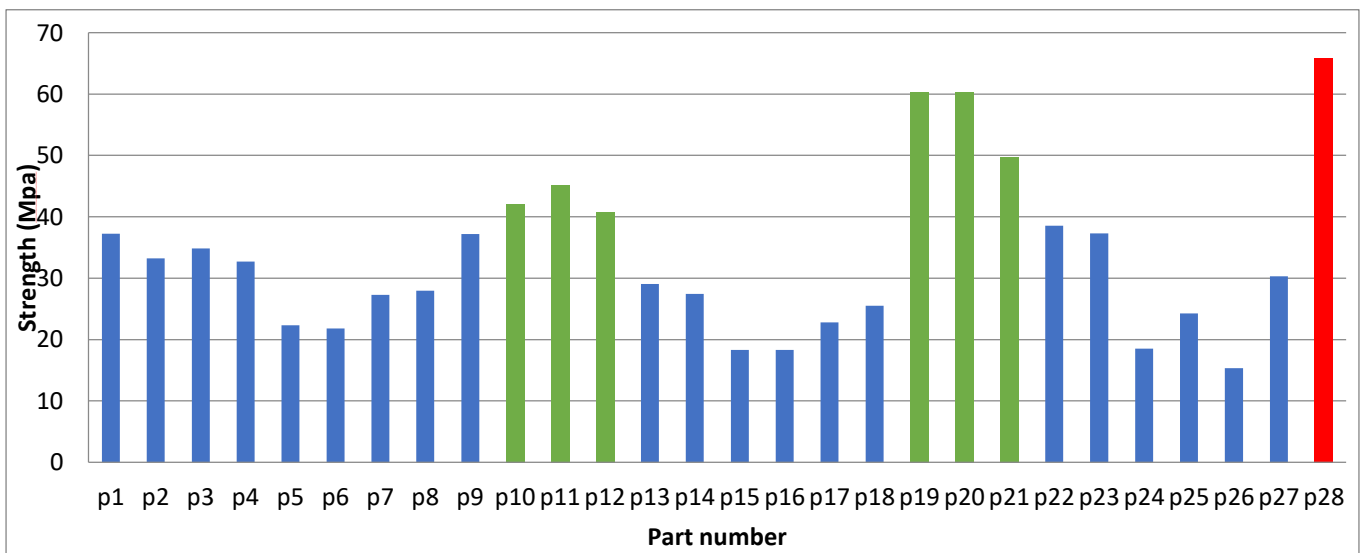


**Figure 4-12:** Strength comparison of 28th part and remaining 27 parts

## CHAPTER 5: CONCLUSION

### 5.1. Conclusion

This paper is all about FDM selected parameters say (Raster angle, Unit cell size, Layer thickness & Extrusion temperature) on compressive strength of primitive scaffold structure. Optimized combination of product process parameters are suggested in result section after experiments. Result shows that strength increases with increase in raster orientation value ranges from 15 degree to 45 degree. While mechanical strength goes on decreasing as the unit cell size increased. Strength also highly depends on layer thickness parameter.

Strength goes on increasing with the increase in layer thickness. Favorable factors as per their respective levels are found on Minitab software which shows value of raster angle= 45 degree, unit cell size= 6 mm, layer thickness= 0.25 mm & extrusion temperature=200. All the values were obtained using “Larger is Better” approach.

### 5.2. Findings of This Study

In this study, raster angle, unit cell size, layer thickness & extrusion temperature were used as input parameters having three different input levels. Taguchi L27 array is used to make different experimental combinations to fabricate samples. Statistical analysis is performed in order to find out the importance of selected process parameters onto mechanical strength that 3D printed part. The effect of these parameters on compressive strength of samples is discussed below:

- All the process-product parameters i.e. extrusion temperature, raster angle, extrusion width & unit cell size have significant impact on mechanical strength of 3D printed samples.
- The interaction between the unit cell size, raster angle, layer thickness & extrusion temperature also posses significant impact on compressive strength.
- Optimal parameters that have maximum compressive strength are found to be raster angle of 45<sup>0</sup>, unit cell size of 6 mm, layer thickness of 0.25 mm and printing temperature of 200<sup>0</sup> C which is depending upon requirements for the compression tests.
- As per previous study, higher infill density (%) insert maximum effect on mechanical strength. Therefore in order to achieve higher infill (%) values, we have used different unit cell size values as the wall thickness of the part was low.
- The porosity of fabricated parts with higher infill density was low which exactly accordance with previous literature is.

### **5.3. Limitations of 3D Printing Machine Available for this Study**

Some limitations were faced during fabrication of 3D printed models using 3D printer machine to carry out this study which are given below:

- As for smaller nozzle diameter, machine yields poor handling which hinders the usage of higher layer thickness values as the extrusion width had taken as percentage of diameter nozzle.
- As layer thickness was taken as percentage of diameter of nozzle & only possible settings of machine for layer thickness ranges between values of 100% of diameter of nozzle to 150% of nozzle's diameter which limits higher layer thickness values.

Even after facing such limitations satisfactory results were obtained and maximum compressive strength for sample. However even facing such limitations the results achieved after compression tests at end were satisfactory and maximum compressive strength for sample-19 was achieved to be 8881.31 N.

### **5.4. Scope of Future Studies**

The scope of future studies is to work on maximum number of FDM parameters to be used such as layer height, printing speed, air gap, infill patterns & build orientation etc. for next parametric studies in order to investigate impact of process-product parameters on mechanical strength of the fabricated samples. Some recommendations for future studies in this field to be conducted are given below:

- The input parameter's levels can be increased such as up to four, five or six levels to minimize the possibility of loss of data during doing of statistical analysis.
- In order to understand the effect on mechanical properties, more FDM parameters can be used such as, layer height, build orientations, air gap, printing speed etc.
- For fabrication of scaffold structure, different materials could be used like ABS, PLA in order to use in different fields.

## REFERENCES

1. Michael Dawoud, Iman Taha, Samy J. Ebeid (2016) Mechanical behaviour of ABS: An experimental study using FDM and injection moulding techniques : 39-45
2. Tobias Maconachie, Rance Tino, Bill Lozanovski, Marcus Watson, Alistair Jones, Chrysoula Pandelidi<sup>1</sup>, Ahmad Alghamdi, Abduladheem Almalki<sup>1</sup>, David Downing, Milan Brandt<sup>1</sup>, Martin Leary (2020) The compressive behaviour of ABS gyroid lattice structures manufactured by fused deposition modelling
3. Diab W. Abueidda <sup>a</sup>, Mete Bakir <sup>a</sup>, Rashid K. Abu Al-Rubb, Jörgen S. Bergström <sup>c</sup>, Nahil A. Sobh <sup>a,d</sup>, Iwona Jasiuk (2017) Mechanical properties of 3D printed polymeric cellular materials with triply periodic minimal surface architectures: 255- 267
4. D. A. de Aquino & I. Maskery & G. A. Longhitano & A. L. Jardini & E. G. del Conte (2020) Investigation of load direction on the compressive strength of additively manufactured triply periodic minimal surface scaffolds :109:771–779
5. Loïc Germaina,<sup>b</sup> Carlos A. Fuentesc, Aart W. van Vuurec, Anne des Rieuxa,<sup>b,\*</sup>, Christine Dupont-Gillainb (2018) 3D-printed biodegradable gyroid scaffolds for tissue engineering applications
6. Michael Dawoud, Iman Taha, Samy J. Ebeid (2016) Mechanical behaviour of ABS: An experimental study using FDM and injection moulding techniques : 39-45
7. M. Afshara, A. Pourkamali Anarakia, H. Montazeriana, J. Kadkhodapour (2016) Additive manufacturing and mechanical characterization of graded porosity scaffolds designed based on triply periodic minimal surface architectures : 6758-136
8. Dario Croccolo , Massimiliano De Agostinis, Giorgio Olmi (2013) Experimental characterization and analytical modelling of the mechanical behaviour of fused deposition processed parts made of ABS-M30 :506-518
9. Sung-Hoon Ahn ,Michael Montero, Dan Odell, Shad Roundy and, Paul K. Wright (2019) Anisotropic material properties of fused deposition modeling ABS : 660-701
10. A K Sood, R K Ohdar, and S S Mahapatra (2009) Parametric appraisal of fused deposition modelling process using the grey Taguchi method
11. R. Anitha, S. Arunachalam, P. Radhakrishnan (2001) Critical parameters influencing the quality of prototypes in fused deposition modeling: 385:388
12. G. Domínguez-Rodríguez, J. J. Ku-Herrera, A. Hernández-Pérez (2018) An assessment of the effect of printing orientation, density, and filler pattern on the compressive performance of 3D printed ABS structures by fuse deposition
13. Caterina Casavola, Alberto Cazzato, Vincenzo Moramarco , Carmine Pappalettere (2016) Orthotropic mechanical properties of fused deposition modelling parts described by classical laminate theory :453-458
14. Hanyin Zhang, Linlin Cai, Michael Golub, Yi Zhang, Xuehui Yang, Kate Schlarman, and Jing Zhang (2016) Tensile, Creep, and Fatigue Behaviors of 3D-Printed Acrylonitrile Butadiene Styrene
15. Gopal K Maharjan, Sohaib Z Khan , Syed H Riza , SH Masood (2018) Compressive Behaviour of 3D Printed Polymeric Gyroid Cellular Lattice Structure : *Eng.*455 012047

16. T J Suteja<sup>1</sup>, A Soesanti<sup>1</sup> (2019) Mechanical Properties of 3D Printed Polylactic Acid Product for Various Infill Design Parameters: A Review
17. Morteza Behzadnasab<sup>1</sup>, Ali akbar Yousefi (2016) Effects of 3D printer nozzle head temperature on the physical and mechanical properties of PLA based product
18. Carmita Camposeco-Negrete (2020) Optimization of printing parameters in fused deposition modeling for improving part quality and process sustainability: 108:2131–2147
19. Deepak Kumar (2019) Optimization the process parameter of FDM 3D printer using Taguchi method for improving the tensile strength: 2455-6211, Volume 7
20. Bharath Vasudevarao<sup>1</sup>, Dharma Prakash Natarajan<sup>2</sup>, Mark Henderson<sup>3</sup>, Ph.D., Anshuman Razdan<sup>4</sup>, Ph.D. (2000) SENSITIVITY OF RP SURFACE FINISH TO PROCESS PARAMETER VARIATION: AZ 85287-5906
21. Umar Shabeer (2021) Strength of 3D printed scaffold structures - a parametric study
22. Uzair Khaleeq uz Zaman<sup>1</sup>, Aamer Ahmed Baqai<sup>2</sup> et al. (2018) Impact of fused deposition modeling (FDM) process parameters on strength of built parts using Taguchi's design of experiments: 101:1215–1226
23. S Restrepo, S Ocampo, J A Ramirez, C Paucar and C Garcia (2017) Mechanical properties of ceramic structures based on Triply Periodic Minimal Surface (TPMS) processed by 3D printing: Series 935 (2017) 012036
24. O. S. Es-Said a , J. Foyos, R. Noorani, M. Mendelson, R. Marloth. A. Pregger (2007) Effect of Layer Orientation on Mechanical Properties of Rapid Prototyped Samples :107-122
25. Ala'aldin Alafaghani, Ala Qattawi et al. (2017) Experimental Optimization of Fused Deposition Modeling Processing Parameters: a Design-for-Manufacturing Approach : 791 – 803
26. Xuan Zhou & Yihua Feng et al (2020) Recent advances in additive manufacturing technology for bone tissue engineering scaffolds: 108:3591–3606
27. Oraib Al-Ketan, Rashid K. Abu Al-Rub (2019) Multifunctional mechanical-metamaterials based on triply periodic minimal surface lattices: A review
28. Nicola CAPPETTI, Alessandro NADDEO and Giuseppe SALERNO. Influence of control parameters on consumer FDM 3d printing. Transdisciplinary Engineering Methods for Social Innovation of Industry 4.0: Proceedings of the 25th ISPE Inc. International Conference on Transdisciplinary Engineering., pages 166–167, 2018.
29. Maskery I et al (2018) Insights into the mechanical properties of several triply periodic minimal surface lattice structures made by polymer additive manufacturing. Polymer 152:62–71
30. Bellehumeur CT, Gu P, Sun Q, Rizvi GM. Effect of processing conditions on the bonding quality of FDM polymer filaments. Rapid Prototyp J 2008;14(2):72–80.
31. Rodríguez-Panes A, Claver J and Camacho A 2018 The influence of manufacturing parameters on the mechanical behaviour of PLA and ABS pieces manufactured by FDM: a comparative analysis Materials 11(8) 1333.

## CERTIFICATE OF COMPLETENESS

It is hereby certified that the dissertation submitted by NS Abdul Moiz Siddiqui, Reg No. **00000318685**, Titled: **Effect of Process-Product Parameters on Strength of 3D Printed Primitive Scaffold Structures** has been checked/reviewed and its contents are complete in all respects.

Supervisor's Name: **Dr. Sajid Ullah Butt**

Signature: \_\_\_\_\_

Date: \_\_\_\_\_